EXPERIMENTAL STUDY OF AN MHD dc PUMP OPERATING AT A HIGHER VOLTAGE

V. A. Golodnyak, Ya. Ya. Zandart,
A. I. Klimenko, I. A. Liepin'sh,
and I. M. Tolmach

UDC 621.313.29:538.4

The capability of an MHD dc pump to operate, in principle, at a higher voltage has been demonstrated in an earlier study [1]. In that study, as well as in others [2, 3], problems concerning the theory and the design of such pumps were also considered.

In this report the authors present the results of an experimental study involving a pump similar to the one in [1], but under more severe conditions of operation (three times higher current and voltage levels, with 10 times higher hydraulic power), which had made it necessary to introduce a few design changes. The theoretical relations have also been refined, by more rigorously accounting for the effects of spatial factors and of the channel shell with soldered-on short-circuiting jumpers.

The pump calculations in [2, 3] were based on a steady flow of liquid metal at a velocity with an x-component only (Fig. 1), on compensation of the induced field, and on a uniform resultant field B with the vector of magnetic induction also having only a component normal to the plane of flow.

As shown in Fig. 1, the channel width is b and its depth is a (inside dimensions); across its length l are spaced electrodes λ wide and at a step t (one behind the other) with jumper connections. The other dimensions necessary for calculating the pump characteristics are also shown in Fig. 1. In pumps of the type considered here the channel length greatly exceeds the stream width. Integrating the equation of motion, we obtain for the pressure head p_a developed by the pump

$$p_a=\frac{1}{b}\int_0^b dy\int_0^l j_y(x,y)B\,dx-\lambda_m\frac{l}{d_h}\frac{\rho v^2}{2}. \tag{1}$$

Here λ_m is the hydraulic drag coefficient and d_h is the hydraulic diameter.

According to expression (5) in [1], the total current across section I–I (Fig. 1) is

$$I=\frac{\gamma ba}{t}\left[\int_0^t j_y(x,0)\,dx+\frac{2\Delta_1}{a}\int_0^t j_{1y}(x,0)\,dx\right]+a\int_0^b j_x(0,y)\,dy+2\Delta_1\int_0^b j_{1x}(0,y)\,dy+2\Delta_1 a j_{1x}(0,0), \tag{2}$$

where j_{1x} and j_{1y} are components of the current density in the shell, and j_x and j_y are components of the current density in the liquid metal.

Since usually $\Delta_1/a \ll 1$, one may assume the electric field intensity in the shell to be uniform over the thickness and equal to the electric field intensity in the liquid metal, so that

$$j_{1y}=\frac{\sigma_1}{\sigma}j_y+\sigma_1 vB;\quad j_{1x}=\frac{\sigma_1}{\sigma}j_x, \tag{3}$$

where σ and σ_1 are the electrical conductivity of the liquid metal and that of the shell material, respectively.

The periodic boundary-value problem of the current-density distribution in a channel with electrodes of finite dimensions has been solved in [4]. There the components of the current density were expressed as

Translated from Magnitnaya Gidrodinamika, No. 2, pp. 105-112, April-June, 1977. Original article submitted August 4, 1976.

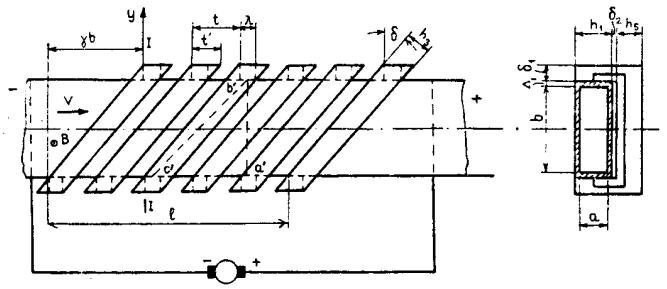

Fig. 1. Channel dimensions (mm): $a = 3.5$; b = 24.8; $\Delta_1 = 0.6$; $\lambda = 3$; t = 13.1; t' = 12.6; $\delta_1 = 5$; $\delta_2 = 0.5$; $h_3 = 5.5$; $h_1 = 4.7$; $h_5 = 5$; $\gamma = 2$; $n = a/b = 0.141$; $l = 890$.

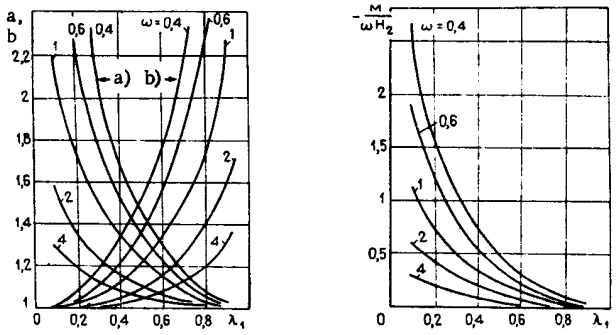

Fig. 2. Graphs for calculating the effect of spatial factors: $\lambda_1 = \lambda/t$, $\omega = b/t$; a) $-T_1/\omega H_2$; b) $T_3/\omega H_3$.

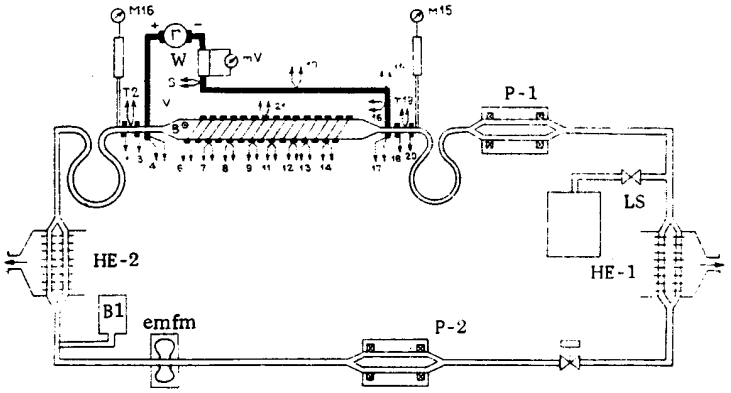

Fig. 3. Basic schematic diagram of the system and location of the test points.

$$j_x(x, 0) = A_1 v_1 + A_2 v_2; \quad j_x(0, y) = A_1 \beta_1 + A_2 \beta_2;$$
$$j_y(x, 0) = A_1 u_1 + A_2 u_2; \quad j_y(0, y) = A_1 \alpha_1 + A_2 \alpha_2. \tag{4}$$

The following symbols for the dimensionless integrals with respect to coordinates $x_1 = x/t$ and $y_1 = y/t$ were also introduced:

$$H_1 = \int_0^1 u_1 dx_1; \quad H_2 = \int_0^1 u_2 dx_1; \quad H_3 = \int_0^1 v_1 dx_1; \quad H_4 = \int_0^1 v_2 dx_1; \quad T_1 = \int_0^\omega \alpha_1 dy_1; \quad T_2 = \int_0^\omega \alpha_2 dy_1; \quad T_3 = \int_0^\omega \beta_1 dy_1; \quad T_4 = \int_0^\omega \beta_2 dy_1. \tag{5}$$

where $\omega = b/t$, and A_1 and A_2 are real constants.

For an isotropically conducting medium we have the relations

$$H_1 = -H_2; \quad H_3 = H_4; \quad T_1 = -T_2; \quad T_3 = T_4. \tag{6}$$

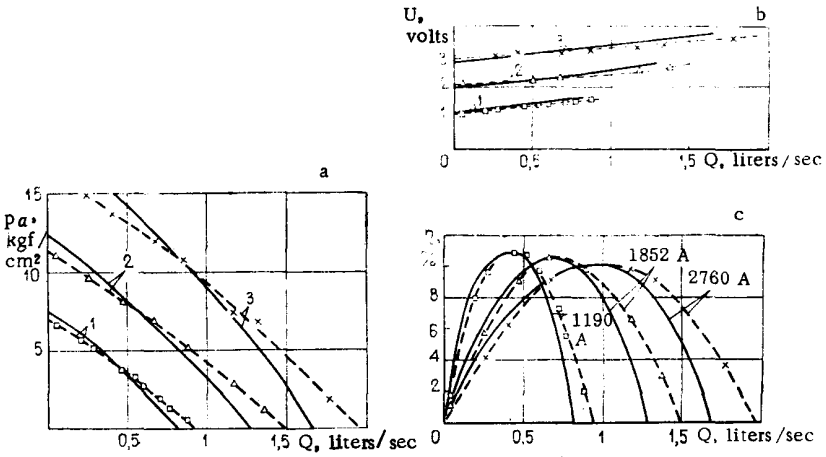

Fig. 4. External characteristics of the pump: a) p(Q) characteristics; b) U(Q) characteristics; c) efficiency η; magnetic induction equal to 0.246 T and sodium temperature 300°C throughout; channel supply current: 1) 1190 A; 2) 1852 A; 3) 2760 A. Solid lines represent calculations; dashed lines represent measurements.

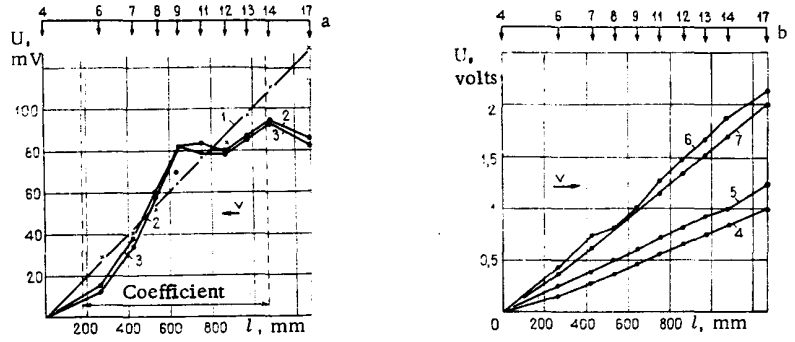

Fig. 5. Distribution of potential along the channel: 1) channel without liquid metal, temperature 28°C and current 22.5 A; 2) operating as a generator, temperature 220°C, flow rate 0.525 liter/sec, pressure head 3.03 bar, current 33.2 A, magnetic induction 0.222 T; 3) operating as a generator at 220°C, 0.45 liter/sec, 3.1 bar, 30 A, 0.282 T; 4) operating as a pump at 255°C, 0.7 liter/sec, 0.43 bar, 795 A, 0.144 T; 5) operating without a field but with a current at 305°C, 1.01 liter/sec, 1.87 bar, 1173 A; 6) operating as a pump at 300°C, 1.08 liter/sec, 1.02 bar, 1415 A, 0.246 T; 7) operating as a lock at 280°C, 0.03 liter/sec, 8.72 bar, 1985 A, 0.194 T.

TABLE 1

Coefficient	a_1, N/(m²·A·T)	10^{-10} b_1, (N·sec)/(m⁵·T²)	10^{-11} c_1, (N·sec²)/m⁸	10^3 a_2, Ω	10^{-3} b_2, N/(m²·A·T)
Experiment	2270	0,81	1,46	0,972	2,2
Calculation	2680	1,08	2,89	1,03	2,67

The constants A_1 and A_2 are determined from Kirchhoff's equations for the contour $a'b'c'$ in Fig. 1 and the external circuit. These equations are

$$\int_{c'}^{a'} \frac{\partial \varphi}{\partial x}\,dx + \int_{a'}^{b'} \frac{\partial \varphi}{\partial y}\,dy - R_J a\left[\int_0^t j_y(x,0)\,dx + \frac{2\Delta_1}{a}\int_0^t j_{1y}(x,0)\,dx\right] = 0;$$
$$U - \frac{1}{\sigma}\int_0^l j_x(x,0)\,dx = 0. \tag{7}$$

Here R_J is the resistance of a jumper and U is the voltage across the end jumpers.

Inserting the solution from [4] for the components of the current density into (1) and (2), with aid of relations (3) and with the notation (4)-(6), we obtain expressions for the p(Q) characteristics and the U(Q) characteristics in the form

$$p_a = a_1 IB - b_1 B^2 Q - c_1 Q^2; \tag{8}$$
$$U = a_2 I - b_2 BQ. \tag{9}$$

Here Q is the volume flow rate of the liquid metal;

$$a_1 = \frac{\gamma\varkappa}{A};\quad b_1 = \frac{\sigma\varkappa l}{ab}\left[1 + r\xi - \frac{\gamma}{(1+\xi)r - T_1/\omega H_2}\,\frac{1+\xi-\xi T_1/\omega H_2}{A}\right];$$
$$c_1 = \frac{\lambda_m l \rho}{2d_h (ab)^2};\quad \varkappa = \frac{M}{\omega H_2} - \frac{T_1}{\omega H_2};\quad a_2 = \frac{a_1}{\sigma\gamma\varkappa};$$
$$b_2 = \frac{\gamma^2}{(1+\xi)r - T_1/\omega H_2}\,\frac{l}{abA}\left(1 + \xi - \frac{\xi T_1}{\omega H_2}\right); \tag{10}$$
$$\xi = \frac{\sigma_1 \cdot 2\Delta_1}{\sigma\Delta};\quad n = \frac{a}{b};\quad r = \frac{R_J \sigma a t}{b};\quad \lambda_1 = \frac{\lambda}{t};$$
$$A = (1+\xi)\left[\frac{\gamma^2}{(1+\xi)r - T_1/\omega H_2} + \frac{T_3}{\omega H_3}\right] + \frac{\xi n}{1-\lambda_1}.$$

The integral quantities $T_1/\omega H_2$, $T_3/\omega H_3$, and $M/\omega H_2$ are determined from the solution to the boundary-value problem, and for practical calculations their values can be taken from the graphs in Fig. 2.

Relations (8)-(10) have been derived on the assumption that v = const and B = const. They yield all characteristics of the pump. For the flow rate Q as well as the current I into the channel and the magnetic induction B given, one can determine the theoretically developed pressure head p_a and voltage U across the channel. The efficiency is then found as the ratio

$$\eta = p_a Q / UI. \tag{11}$$

The object of this study is now to compare calculations according to expressions (8) and (9) with experimental results, as well as to check whether the design of individual structural components and the values of their parameters, especially the jumper resistance and the lineal resistance of the channel, are correct.

The pump prototype was built with the following structural characteristics. The rectilinear pump channel was a pipe of rectangular cross section 24.8 × 3.5 mm in size and 0.6 mm in wall thickness. The channel material was grade 1Kh18N10T stainless steel. Copper jumpers shown in Fig. 1 were soldered to the channel over a length of 890 mm. The channel, together with a water-cooled rail above it for compensating the reaction of to the longitudinal current, was placed in the gap of a C-shape magnet system.

The effective jumper resistance R_J is determined from the geometry (Fig. 1) and is

$$R_J = R_E + R_{JS} = \frac{4\Delta_1}{\sigma_1 a l (1+\lambda_1)} + \frac{1}{\sigma_J}\left[\frac{\delta_1}{\lambda_1 h_1} + \frac{h_1 + 2\delta_2}{\lambda\delta_1} + \frac{h_5}{t\delta_1} + \frac{\sqrt{(\gamma b)^2 + (b + 2\Delta_1 + 2\delta_1)^2}}{h_3 h_5}\right], \tag{12}$$

where σ_J is the electrical conductivity of the jumper material, R_E is the resistance of an electrode (through the channel), and R_{JS} is the resistance of a jumper alone.

The lineal resistance R_L of the channel with soldered-on jumpers can be calculated with the aid of expressions (9), (10), (12), letting the electrical resistivity of the liquid metal be equal to zero. For this case expression (9) yields

$$\frac{1}{R_L}=\frac{2\sigma_1\Delta_1 b}{l}\left(1+n+\frac{2\Delta_1}{b}+\frac{b\gamma^2}{b+\sigma_1 2\Delta_1 t R_{JS}}\right). \tag{13}$$

The experiment was performed with a sodium system at the Institute of Physics, Academy of Sciences of the Latvian SSR.

The pump was connected into the system through compensator loops of tubing each 20 mm in diameter and about 1.5 m long (Fig. 3).

These loops had made it possible to reduce the current in the shunt paths of the system and, at the same time, to compensate for the thermal expansion of the conduits. The thermal operating conditions were maintained by heat exchangers HE-1 and HE-2, while the pump was hydraulically loaded by two cylindrical induction pumps P-1 and P-2.

The magnet system of the pump was energized from a model P-102 dc generator; the channel was supplied from a model NG-2500/5000 motor–generator set.

During the experiment we measured the flow rate, the pump inlet and outlet pressure, the potential distribution and the temperature distribution along the channel, the voltage drop across a jumper, the source current, the shunt current, and the magnetizing current. The flow rate of the liquid metal was checked with an electromagnetic flowmeter. The pressures were measured with standard manometers M15 and M16 through an argon pad.

The distributions of potential and temperature were measured with the leads of Chromel–Alumel thermocouples which had been embedded at the jumper ends. One electrode of such a thermocouple (the Chromel wire) was used for measuring the potential. All thermocouples were brought out to a model TPP-20 dial switch. The voltage drop was measured with a model M1106 instrument and the temperature was measured with three model ÉPV-2-06 potentiometers.

The current in the shunt paths was measured at the inlet to and at the outlet from the pump channel. For this purpose, copper washers had been soldered onto a conducting tube over a base length of 81 mm, the current then being calculated from the voltage drops (points 1-3 and 18-20 in Fig. 3). The pump supply current I was calculated as the difference between the source current and the shunt current.

The induction in the gap of the magnet was determined from the magnetization curve of magnetic induction versus magnetizing current, which had been plotted in a separate test.

All essential data were obtained at 300°C, the temperature of liquid sodium, at which the channel walls become wettable rather fast and remain in this condition steadily enough so that any contact resistances vanish.

A large amount of data was obtained by measurement of the external characteristics of the pump at various levels of the source current and of the magnetic induction in the gap. Altogether 167 operating points were recorded. Each characteristic was plotted in the direction of increasing and decreasing flow rate. As an example, in Fig. 4 we show three experimental p(Q) characteristics together with the corresponding U(Q) and η(Q) characteristics.

The results have been evaluated in terms of a representation of the pump channel characteristics in the form of two relations according to the method proposed in [5] [differing from relations (8) and (9) only in the grouping of terms]:

$$\frac{p_a}{IB}=a_1-b_1\frac{BQ}{I}-c_1\frac{Q^2}{IB}; \tag{14}$$

$$\frac{U}{I}=a_2+b_2\frac{BQ}{I}. \tag{15}$$

For calculating the dimensional coefficients a_i and b_i, we selectively used in the evaluation 29 experimental points at which the temperature of the liquid metal had been 300°C.* The values of these coefficients based on the test results are given in the first row of Table 1, while those based on calculations according to expressions (10) for the metal at 300°C are given in the second row.

The graphs in Fig. 4 indicate a satisfactory agreement between calculation and experiment, the error of both sets of values not exceeding 15%. During the experiment the voltage across the pump channel reached 3.6 V and the supply current reached 2900 A, while the maximum pressure head, flow rate, and channel efficiency were, respectively, $16 \cdot 10^5$ N/m^2, $2 \cdot 10^{-3}$ m^3/sec, and 11.8%. The Hartmann number reached the value 115 and the Reynolds number reached the value $2 \cdot 10^5$.

If a current is sent along a pump channel not containing any metal, then a measurement of the longitudinal distribution of potential will, when the latter is found to be linear, yield the linear channel resistance.

The distribution of potential at a channel temperature equal to 28°C and a current equal to 22.05 A is shown in Fig. 5 (curve 1). The lineal resistance R_L was calculated from the voltage drop between the two test points 6 and 12 (Fig. 3). It was found to be $R_L = 4.77 \cdot 10^{-3}$ Ω/m. Calculations according to expression (13) yielded $R_L = 4.84 \cdot 10^{-3}$ Ω/m, with an error smaller than 1.5% relative to the measured value. Inasmuch as the effective jumper resistance appears in relation (13), one may conclude that this component of the channel structure has been designed correctly.

On the diagram in Fig. 5 are shown the distributions of potential along the pump channel in various modes of operation. The generator modes of operation (curves 2 and 3) are characterized by a dip of potential at the inlet where liquid metal enters the channel.

Because of the low current levels in these modes of operation, the electrodynamic forces should have had almost no effect on the flow mode. Since the external pumps P-1 and P-2 (Fig. 3) were known beforehand to produce strong fluctuations on the flow rate, this dip of potential could probably be attributed to a lengthwise nonuniform stream velocity.

In no operating mode, except as a lock, was there evident any appreciable temperature variation along the channel. In the locking mode, especially with high supply currents, the temperature of the metal rose steeply with time.

Essential in the theory of this pump is the problem of assuming for relations (8) and (9) a uniform resultant magnetic induction in the gap. In reality, there exists some nonuniformity in the distribution of the magnetic induction over the area of the gap, which is due to a slight taper of the magnetic field from the center to the edge of the gap, as well as due to the field of the "armature" reaction of the currents flowing through the liquid metal, the jumpers, and the compensator rail. In the derivation of the theoretical relations we have assumed that the fields of the currents through these structural components fully compensate one another and that the resultant magnetic induction is equal to the mean-over-the-(gap) area intrinsic induction of the magnet, depending on the excitation current only.

With aid of our experimental results and on the basis of the theoretical relations, we can now estimate the actual magnetic induction in the channel. For simplifying the calculations, we will assume that all parameters are uniformly distributed along channel.

The current through a jumper in Eqs. (7) will be expressed as

$$I_J = a\int_0^t j_y dx + 2\Delta_1 \int_0^t j_{1y} dx$$

and, with aid of relations (3) as well as on the basis of the foregoing assumption, we write

$$I_J = at[(1+\xi) j_y + \sigma\xi vB].$$

Applying Ohm's law to j_y and eliminating $\partial\varphi/\partial y$ from expression (7) yields

$$(1+\xi)\gamma E_x + \frac{I_J}{\sigma ta}(1+r+r\xi) + vB = 0.$$

*The calculations were made by R. Pesina according to the standard program for evaluation of experimental data developed at the Optimal Processes Laboratory of Khar'kov State University.

From the distribution of potential along the channel we determine E_x according to the relation $E_x = U_{12-6}/l_{6-12}$, and from the voltage drop across the slanted jumper segment we determine the jumper current $I_J = U_{9-21}/R_S$, where R_S is the resistance of the slanted jumper segment (Fig. 1) and U_{12-6} and U_{9-21} are the potential differences between points 12-6 and points 9-21 (Fig. 3), respectively. We finally have

$$B=\frac{1}{v}\left[(1+\xi)\gamma\frac{U_{12-6}}{l_{6-12}}-\frac{U_{9-21}}{R_S\sigma ta}(1+r+r\xi)\right]. \quad (16)$$

In our particular case we determine the true magnetic induction according to expression (16) with the flow rate (velocity v) known. All data needed for this calculation are given in Fig. 5. The magnetic induction thus determined (corresponding to curves 4-7 in Fig. 5) differs by not more than 10% from that determined on the basis of the excitation current, which is quite within the experimental accuracy. One may, therefore, conclude that the currents through the channel have no demagnetizing effect.

Theoretical problems requiring a further thorough study include that of accounting for losses within the triangular end zones of the channel and that of calculating more reliably the hydraulic losses in the channel.

On the whole, the theoretical relations shown here may be regarded as agreeing, within a 15% accuracy, with the experiment and thus being suitable for engineering calculations.

LITERATURE CITED

1. I. T. Alad'ev, V. A. Mukhin, V. E. Strizhak, S. V. Teplov, and I. M. Tolmach, "Experimental study of an MHD dc machine with segmental electrodes," Magnitn. Gidrodinam., No. 1, 64-72 (1971).
2. V. A. Golodnyak, A. E. Sinel'nikova, and I. M. Tolmach, "Analysis of the fundamental relations in an electromagnetic dc pump operating at a higher voltage," in: Proceedings of the Fifth Tallin Conference on Electromagnetic Flowmeters and Electrical Engineering of Liquid Metals [in Russian], Vol. 4, Tallin (1971), pp. 96-113.
3. B. B. Volchek, G. M. Gekht, and V. A. Golodnyak, "Effect of a finite segmental electrode on the efficiency of a dc pump operating at a higher voltage," in: Eighth Riga Conference on Magnetohydrodynamics [in Russian], Vol. 2, Riga (1975), pp. 97-99.
4. I. M. Tolmach and N. N. Yasnitskaya, "Hall effect in a channel with segmental electrodes," Izv. Akad. Nauk SSSR, Énerget. Transport, No. 5, 91-104 (1965).
5. D. S. Kovner, L. M. Titov, and Yu. P. Ushakov, "Some problems in the analysis of experimentally established characteristics of channels in MHD dc conduction machines," Izv. Vyssh. Uchebn. Zaved., Énerget., No. 8, 90-94 (1970).